Clays and Clay Minerals, Vol. 49, No. 4, 318–332, 2001.

COMPARISON OF EVOLUTION OF TRIOCTAHEDRAL CHLORITE/BERTHIERINE/SMECTITE IN COEVAL METABASITES AND METAPELITES FROM DIAGENETIC TO EPIZONAL GRADES

M. P. MATA[1], G. GIORGETTI[2], P. ÁRKAI[3] AND D. R. PEACOR[4]

[1]Department of Geology, The University of Cádiz, Pol. Rio San Pedro, 11510, Pto Real, Cádiz, Spain
[2]Department of Earth Sciences, University of Siena, Via Laterina, 8, 53100 Siena, Italy
[3]Laboratory for Geochemical Research, Hungarian Academy of Sciences, H-1112 Budapest, Budaoersi út 45, Hungary
[4]Department of Geological Sciences, The University of Michigan, Ann Arbor, Michigan 48109, USA

Abstract—The evolution of texture, structure and chemical composition of chloritic clays in coeval pairs of metabasites and metapelites of a prograde sequence from the Bükk Mountains has been investigated using electron microscopy techniques. Samples are from the Bükkium (innermost Western Carpathians, Hungary) that underwent Alpine metamorphism, ranging from late diagenesis to epizone for pelites and from prehnite-pumpellyite to greenschist facies for the metabasites.

Although bulk-rock compositions, textures and primary minerals are different, chlorite evolved at similar rates in coeval metabasites and metasediments, but along different paths. The principal similarities in the prograde sequence are a decrease in the percentage of interstratified material in both dioctahedral and trioctahedral phyllosilicates and increase in thicknesses of chlorite and illite crystallites. The principal difference is in the type of interstratification in chlorite, with berthierine in metapelites, and smectite (saponite) in metabasites, although smectitic mixed layers also occur in the former. The evolution of trioctahedral phyllosilicates is marked by a decrease in the number of mineral species with increasing grade, chlorite, *sensu stricto*, being the only trioctahedral mineral at higher grades. This is consistent with the trend in reaction progress where both metastable systems (metabasites and metapelites) tend toward the same end-member, thermodynamically stable chlorite, as well as texture (crystal size), and where all intermediate states are metastable, and determined by the Ostwald step rule.

Key Words.—AEM, Berthierine, Bükk Mountains, Chlorite, Low-grade Metamorphism, Reaction Progress, Smectite, TEM, XRD.

INTRODUCTION

Evolution of phyllosilicates in rocks ranging in grade from diagenesis to the greenschist facies has been studied extensively in the last few years, with emphasis on dioctahedral smectite–illite–muscovite transformations and evolution of the illite crystallinity index in metapelitic rocks (Merriman and Peacor, 1999; Merriman and Frey, 1999 and references therein). In addition to illite-muscovite, chlorite is a widespread phyllosilicate in diagenetic and low-grade metamorphic rocks (Frey, 1987; Laird, 1988; Robinson and Merriman, 1999; Schiffman and Day, 1999; Robinson and Bevins, 1999). The evolution of trioctahedral phyllosilicates from smectite to chlorite has received increasing attention recently. Most studies of the mineralogical evolution of trioctahedral phases have dealt with regionally metamorphosed or hydrothermally-altered mafic rocks (for recent reviews see Árkai and Sadek Ghabrial, 1997; Robinson and Merriman, 1999; Alt, 1999; Schiffman and Day, 1999 and references therein) where chlorite occurs as an alteration product of ferromagnesian silicates and glass. In metapelites, chlorite appears as a detrital or authigenic/metamorphic mineral and its abundance is conditioned by bulk-rock composition (Hillier, 1993; Jiang and Peacor, 1994a, b; Dalla Torre *et al.*, 1996; Schmidt *et al.*, 1999).

Studies of metapelites and metabasites show that structural, textural and compositional changes in chlorite are a function of metamorphic grade (temperature). In general, the proportion of mixed-layered components decreases with increasing metamorphic grade (Jiang and Peacor, 1994b; Schiffman and Day, 1999; Robinson and Bevins, 1999; Alt, 1999 and references therein). The saponite–corrensite–chlorite series of transitions has been described in both metapelites and metabasites. Corrensite has been interpreted in two ways: (1) as alternating layers of chlorite-saponite/vermiculite, implying that there is a continuous sequence of mixed-layered phases between pure smectite and chlorite; or (2) as a phase with unique structure and composition. Chlorite crystallinity (ChC), which is analogous to illite crystallinity (IC), has also been found to be a reliable tool in the determination of relative reaction progress in low-grade rocks (Árkai, 1991). Árkai *et al.* (1995) confirmed the applicability of ChC for monitoring diagenetic through incipient-metamorphic grades of fine-grained clastic metasediments and Árkai and Sadek Ghabrial (1997) demonstrated that ChC can also be used to determine relative metamorphic grade (reaction progress) in metabasites. The ChC (similarly to IC) seems to be controlled mainly by the amounts of mixed-layered components at lower (diagenetic and lower-anchizonal) grades and

Copyright © 2001, The Clay Minerals Society

https://doi.org/10.1346/CCMN.2001.0490406 Published online by Cambridge University Press

is principally a function of mean crystallite thickness (size) at higher anchizonal and epizonal grades (Árkai and Tóth, 1990; Árkai and Sadek Ghabrial, 1997). Berthierine has been inferred to be a precursor of chlorite in diagenetic rocks. Although mixtures of berthierine with chlorite at very fine scales may easily escape detection during routine mineralogical analyses, intercalation of berthierine in chlorite has been described by several investigators (Lee and Peacor, 1983; Ahn and Peacor, 1985; Amouric *et al.*, 1988; Hillier and Velde, 1992; Jiang *et al.*, 1992; Hillier, 1994) and such materials have been inferred to be precursors of pure chlorite in diagenetic rocks.

The general trends of evolution of trioctahedral phyllosilicates in both metapelites and metabasites are well known. The prograde changes involve metastable states (*e.g.* mixed layering, small crystal size; see Essene and Peacor, 1995) that depend on kinetic factors which influence reactions between starting materials and more stable states. The bulk compositions, textures and original mineral assemblages of sediments and basaltic rocks are very different. The rates of reaction toward the stable assemblages with relatively small numbers of large, homogeneous chlorite crystals may therefore be very different. Morse and Casey (1988) showed that intermediate states in such systems are controlled by rates of reaction between a large number of possible successive intermediate states, in terms of the Ostwald step rule. The state, *i.e.* the reaction progress of trioctahedral clay minerals in metapelites and metabasites formed at the same grade (temperature), may therefore be very different, as has been demonstrated for some dioctahedral clay minerals (Masuda *et al.*, 1996; Li *et al.*, 1997). A comparative study of evolution of trioctahedral clay minerals in metabasalts and metasediments affected by the same metamorphic conditions has not been carried out to date, perhaps in part because continuous sequences that contain both metapelites and metabasites subjected to simple prograde relations are rare.

We have therefore carried out a study of evolution of coeval pairs of metabasites and metapelites to determine the similarities and differences in reaction progress in trioctahedral phyllosilicates. The selected pairs of rocks cover a range of regional metamorphism from prehnite-pumpellyite to greenschist facies (metabasites) and diagenesis to epizone (metapelites) from the Bükkium megatectonic unit (Bükk and Uppony Mountains, NE Hungary). Metamorphic grade was determined on the basis of mineral facies and IC index, respectively (Árkai, 1983; Árkai *et al.*, 1995). Samples have been studied using a variety of techniques, with emphasis on X-ray powder diffraction (XRD) and transmission and analytical electron microscopy (TEM/AEM) in order to determine the evolution in texture, composition and structure of the trioctahedral minerals.

This report is the second of a two-part series. In the first part, we emphasized comparison of ChC indices, as calculated by XRD, and TEM- and XRD-determined thickness values, as well as the relations between ChC and chlorite chemistry. These relations showed that despite differences in composition, mineral assemblages and textures, ChC values of coeval metapelites and metabasites changed in a regular way with increase in grade, and with nearly identical values in coeval pairs (Árkai *et al.*, 2000). In the present paper we describe the evolution of texture, composition and structure of trioctahedral phyllosilicates in detail, emphasizing the mineralogical relations, as a function of reaction progress in pairs of metasedimentary and metabasic rocks over a broad range of grades.

MATERIALS

Samples were described in detail by Árkai *et al.* (2000) and thus are only briefly characterized here. All samples came from the innermost tectonic units of the Western Carpathians (Figure 1a). This area was affected by regional metamorphism from deep diagenesis to epizonal grade, as determined by IC values of metapelites and mineral parageneses in metabasites. Figure 1b displays the main geological and tectonic features of the Bükk and Uppony Mountains where the samples originated. Tectonic and petrogenetic results have been summarized previously in Árkai (1983, 1991), Kovács (1989), Downes *et al.* (1990), Árkai *et al.* (1995), Sadek Ghabrial *et al.* (1996), Kovács *et al.* (1996–97) and Árkai *et al.* (2000). The four sequences studied were: Darnó Hill (DH), Szarvskö complex (SZ), Eastern Bükk Mountains (EB) and Uppony Mountains (UM), with metamorphic grades and mineralogy as determined by XRD (Árkai *et al.*, 2000) listed in Table 1. In the Darnó Hill series, Middle Triassic pillow basalts showing ocean-floor hydrothermal metamorphism with prehnite-pumpellyite facies assemblages are interbedded with pelitic sedimentary rocks that were only diagenetically altered. The Szarvaskö complex consists of a Jurassic dismembered, MORB-type, ophiolite-like ultrabasic–basic–(acidic) sequence and clastic sedimentary rocks (Árkai, 1983). The meta-igneous rocks display prehnite-pumpellyite facies assemblages and the alteration of the fine-grained clastic sedimentary rocks varies in grade from late diagenesis to lower anchizone. In the Eastern Bükk Mountains, the Triassic (Carnian) basic volcanic complex suffered pumpellyite-actinolite facies orogenic metamorphism, whereas the transformation of the Ladinian stratovolcanic formation, built up by lavas and predominantly fine-grained pyroclastic rocks of mostly andesitic compositions, reached the chlorite zone of the greenschist facies. The Carnian fine-grained clastic formation that separates the above-mentioned magmatic units was metamorphosed under transitional anchi- to epizonal conditions. The Uppony

https://doi.org/10.1346/CCMN.2001.0490406 Published online by Cambridge University Press

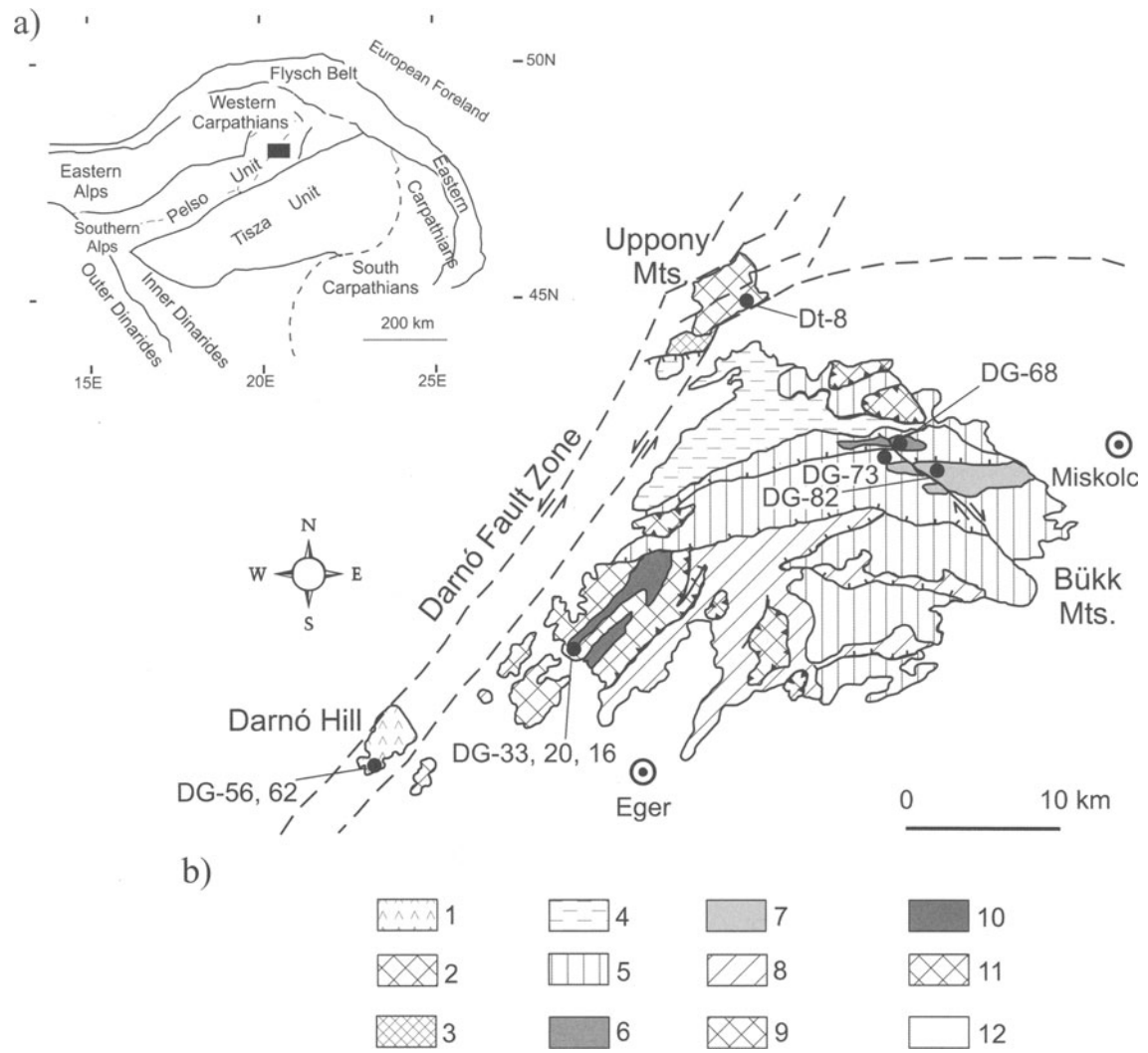

Figure 1. (a) Tectonic setting of the Bükkium and the South-Gemer Unit within the Alp-Carpathian-Dinaric framework. (b) Geological sketch map of the Bükk and Uppony Mountains after Kovács (1989), simplified, with the locations of the samples investigated. Key: 1=Meliaticum: Triassic and Jurassic metabasites and metasediments of the Darnó Hill, SW-Bükk Mts.; 2=Uppony Paleozoic [Ordovician(?)–Middle Carboniferous]; 3=Gosau-type Senonian conglomerates in the Uppony Mts; 4–8: Bükk Parautochthon: 4=Upper Paleozoic; 5=Triassic sedimentary formations; 6=Ladinian meta-andesite and tuffs; 7=Carnian metabasalt, metarhyolite and their tuffs; 8=Jurassic sedimentary rocks; 9–10: Szarvaskö-Mónosbél Nappe: 9=Jurassic sedimentary rocks; 10=Jurassic incomplete, ophiolite complex; 11=Kisfennsík ('Little Plateau') Nappe (Triassic); 12=Cenozoic.

Mountains (UM) are built up by mostly epizonal Paleozoic rocks. Epizonal slate and metasandstone samples intercalated with greenschist-facies metabasalts from borehole Dt-8 were selected for this study.

All of the Mesozoic and Paleozoic formations of the Bükkium and the investigated nappes of the South Gemer (Meliata) Unit suffered low to transitional low-intermediate pressure-type Alpine orogenic metamorphism in the time span between the Upper Jurassic and Middle Cretaceous, *i.e.* between the eo-Hellenic and Austrian phases of the Alpine cycle (Árkai *et al.*, 1995).

SAMPLES AND ANALYTICAL TECHNIQUES

On the basis of previous XRD, EMP and bulk-rock and chemical data, 11 samples were studied by scanning electron microscopy (SEM) and TEM. Sample identifications, metamorphic grade as determined by IC, mineral facies, and mineral assemblages are listed in Table 1.

The SEM observations included back-scattered electron (BSE) imaging of polished thin-sections and ion-milled TEM specimens using a HITACHI S-3200N SEM, equipped with a Noran X-ray energy-

https://doi.org/10.1346/CCMN.2001.0490406 Published online by Cambridge University Press

Table 1. Rock samples investigated. Abbreviations of mineral names after Bucher and Frey (1994) except for Chl-Sm = chlorite-smectite mixed-layered mineral. Metasedimentary rock units in italics.

Seq.	Sample	Metamorphic grade	Bulk mineralogy (petrographic microscopy, XRD and EMPA)
DH	DG-56	Prh-Pmp	Qtz Ab Chl Chl/Sm Cpx Pmp Prh Cal Mag Hem Ilm Ttn Ap
DH	*DG-62*	*Diag. (I.C.)*	*Qtz Ab Ill-Ms Chl Py*
SZ	DG-33	Prh-Pmp	Qtz Ab Ill-Ms Chl Chl-Sm Cpx Ep Pmp Prh Cal Mag Ilm Ttn Ap
SZ	DG-16	Prh-Pmp	Qtz Ab Ill-Ms Chl Cpx Act Pmp Prh Cal Mag Hem Rt Ilm Ttn Ap
SZ	*DG-20*	*Diag. (I.C.)*	*Qtz Ab Ill-Ms Chl Cal*
EB	DG-82	Pmp-Act.	Qtz Ab Ill-Ms Chl Cpx Act Ep Pmp Cal Hem Ilm Ttn Ap
EB	*DG-73*	*Anchiz. (I.C.)*	*Qtz Ab Ill-Ms Chl Chl-Sm Cal Py Rt*
EB	DG-68	Greenschist	Qtz Ab Ill-Ms Chl Cal Hem Rt Ilm Ap
UM	*Dt-8, 118*	*Epiz. (I.C.)*	*Qtz Ab Kfs Ill-Ms Chl Ank Py Rt*
UM	Dt-8, 129	Greenschist	Qtz Ab Kfs Ill-Ms Chl Stp Cal Ank Mag Hem Rt
UM	*Dt-8, 207.5*	*Epiz. (I.C.)*	*Qtz Ab Kfs Ill-Ms Cal Chl Py Hem Rt*

dispersive spectra (EDS) analytical system, and operated at 20 kV at the University of Michigan. Following optical and BSE examination, specimens were removed from thin-sections, ion-milled, and carbon coated. The TEM observations and AEM analyses were obtained using a Philips CM12 scanning-transmission electron microscope (STEM), operated at an accelerating voltage of 120 kV and beam current of 10 μA at the University of Michigan. Lattice-fringe images of phyllosilicates were obtained using 001 reflections. Initial focus was controlled manually by minimizing contrast, and images were taken at overfocus conditions (1000 Å). X-ray energy-dispersive spectra were obtained using a Kevex Quantum detector. A raster of 2000 × 2000 Å (as maximum size) in scanning mode was used to minimize alkali diffusion and volatilization. The AEM-determined formulae were calculated from spectra using k-values obtained from standards of paragonite, muscovite, albite, clinochlore, fayalite, rhodonite and titanite, following the procedure of Jiang *et al.* (1990).

RESULTS

BSE observations

The BSE images of coeval pairs illustrate the textural evolution of trioctahedral phyllosilicates from diagenesis to epizone in both metasediments and metabasalts at a scale intermediate to that of hand specimen and TEM. Minerals were identified in part through EDS analyses.

Lower-grade metabasites and diagenetic pelites. Figures 2a and 2b are BSE images of thin-sections of coeval low-grade metabasalt and metapelite. Chlorite in low-grade metabasites, from the DH and SZ sequences, occurs with fine-grained acicular, lath-shaped plagioclase crystals that are completely albitized, and amphibole crystals. Cross-cutting veins occur which are composed of 'chlorite' (when enclosed within inverted commas, as 'chlorite', the term refers to trioctahedral material consisting largely of chlorite, but perhaps with a mixed-layer component), quartz, prehnite and pumpellyite. 'Chlorite' (Figure 2a) occurs as a secondary mineral with actinolitic amphibole along fractures in pyroxene, in the fine-grained groundmass surrounding altered phenocrysts, and filling veins and fractures.

The two low-grade metapelites from the DH and SZ sequences are similar, and are composed of coarse-grained quartz, albite, 'chlorite', muscovite and chlorite-mica stacks which have the appearance of detrital grains, with minor apatite, titanite, zircon, pyrite and rutile (Figure 2b). Surrounding those clasts is a fine-grained matrix, with individual grains often not resolvable by SEM, but EDS analyses imply that it consists primarily of phyllosilicates, including major illite and minor chlorite. In both of the studied metapelites, 'chlorite' occurs in two modes: (1) as large chlorite-mica stacks, up to 50 μm in size, where 001 planes of chlorite and mica are parallel to subparallel (some of the chlorite-mica stacks are weakly deformed, with bent layers); and (2) as small grains, <5 μm in size, in the matrix.

Pumpellyite-actinolite and greenschist-facies metabasites and anchi-, epizonal metapelites. Figures 2c and 2d are BSE images of thin-sections of coeval pairs of epizonal metabasite and metapelite, respectively. Figure 2c shows that albite, muscovite and chlorite occur as μm-sized crystals with minor titanite, calcite and pyrite in the metabasite. Chlorite is abundant as thick crystals and irregular aggregates, commonly associated with calcite, albite and pyrite. Thick muscovite crystals are also present.

The texture of epizonal metapelites (Figure 2d) is characterized by intergrown crystals of quartz, phyllosilicates (chlorite and muscovite), albite, rare K-feldspar and in a well-foliated structure. Rutile and pyrite are minor constituents. Foliation is largely defined by parallel to subparallel packets of phyllosilicates up to ~1 μm thick. No coarse chlorite-mica stacks were detected in high-grade samples. Chlorite in epizonal rocks thus appears as intergrowths of thick crystals with muscovite and quartz in a typical metamorphic texture of interlocking grains. Metapelites from the Szarvaskö Complex and borehole Dt-8 show abundant pore-space. Most grain boundaries are serrated, embayed and rounded, suggest-

https://doi.org/10.1346/CCMN.2001.0490406 Published online by Cambridge University Press

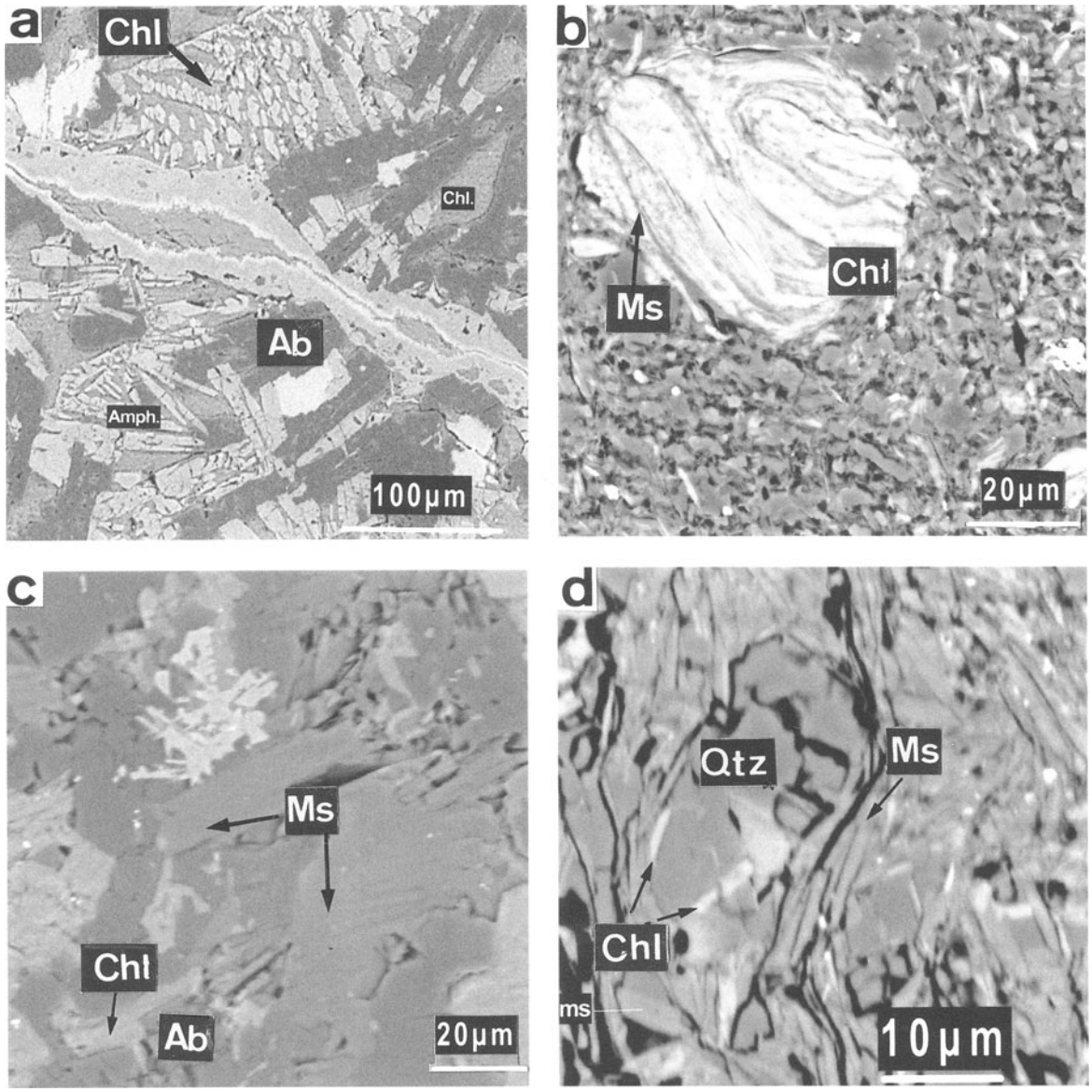

Figure 2. BSE images of pairs of rocks of the same metamorphic grade: (a) metabasalt of prehnite-pumpellyite facies (sample DG-56); (b) diagenetic metapelite (sample DG-20); (c) greenschist-facies metabasalt (sample DT-8, 129 m); and (d) epizonal metapelite (DG-73). Ms: muscovite, Chl: chlorite; Ab: albite; Qtz: quartz.

ing that the surfaces have suffered some dissolution and crystallization via pore-fluids. Sandstone sample Dt-8 207.8 m has feldspar domains consisting of albite cores surrounded by K-Ba feldspar, with rims consisting primarily of K-feldspar. Calcite and chlorite are commonly associated with this feldspar assemblage. Monazite occurs as 50 µm sized euhedral crystals. These relations imply that this sample has been affected by fluids.

The overall appearance of BSE images shows that lower-grade pelites have a texture typical of sedimentary rocks, with sharply defined detrital grains in a fine-grained matrix rich in phyllosilicates. Higher-grade metapelites display typical foliated, metamorphic texture, implying dissolution and recrystallization of grains of lower-grade rocks. Both lower- and higher-grade metabasites retain a texture typical of igneous rocks, with more or less altered phenocrysts in a fine-grained matrix.

TEM observations

Lower grade metabasites. 'Chlorite' is the main phyllosilicate in the pillow lavas of Darnó Hill and the Szarvaskö complex. It occurs as packets with random orientation sometimes enclosed by albite crystals and showing weak signs of deformation that are imaged as intracrystalline kink bands. 'Chlorite' crystals occur both as parallel packets showing straight layers with a

https://doi.org/10.1346/CCMN.2001.0490406 Published online by Cambridge University Press

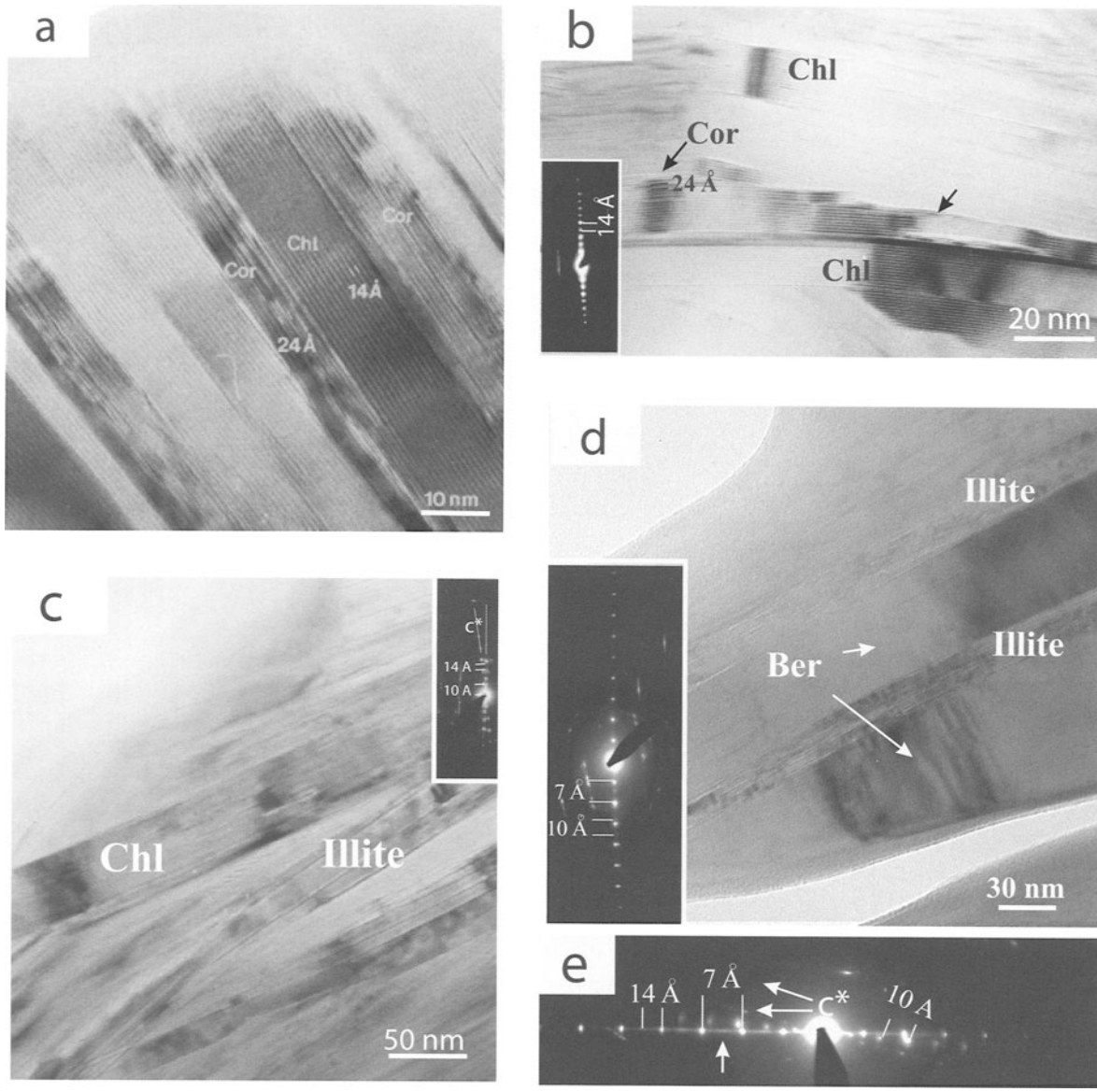

Figure 3. (a) Lattice-fringe image of corrensitic units and chlorite crystals of sample DG-56, Darnó Hill metabasalt. (b) Lattice-fringe image of sample DG-16 with discrete chlorite crystals and corrensitic units. The inset SAED pattern shows 001 reflections with $d(001)$ values of 14 Å. (c) Low-resolution TEM image of metapelite DG-20 of the diagenetic zone showing illite and chlorite crystals. The inset SAED pattern shows 001 reflections with $d(001)$ = 10 Å and $d(001)$ = 14 Å. (d) TEM image of sample DG-20 showing packets of berthierine crystals parallel to illite crystals. The inset SAED pattern shows 001 reflections with $d(001)$ = 7 Å and $d(001)$ = 10 Å. (e) Typical SAED pattern of sample DG-20 with parallel 14 and 7 Å reflections with streaking along c* (arrow) and 10 Å reflections.

few defects (Figure 3a) and as curved crystals with low-angle contacts and abundant layer terminations (Figure 3b). The TEM images show that mixed layering of saponite/vermiculite layers in 'chlorite' packets is common in the pillow lava metabasalts of the DH and SZ sequences. Collapsed smectite has wavy 10 Å fringes but locally (*e.g.* in sample DG-56, Figure 3a) discrete corrensitic units up to 100 Å thick occur. In Figure 3a discrete chlorite crystals, up to 200 Å thick, are separated by corrensitic units <100 Å thick. Discrete, <120 Å, thick packets of corrensite were also observed, but only rarely. Lattice-fringe images of mixed-layer Chl/Sm commonly show defects and layer terminations. The SAED patterns of chlorite from low-grade metabasites show 14 Å periodicity and disordered stacking sequences as seen by streaking and lack of periodicity in reflections with $k \neq 3n$. Figure 3b shows a lattice-fringe TEM image of sample DG-16, metadiabase from the Szarvaskö complex. Chlorite occurs as defect-free or curved crystals with

https://doi.org/10.1346/CCMN.2001.0490406 Published online by Cambridge University Press

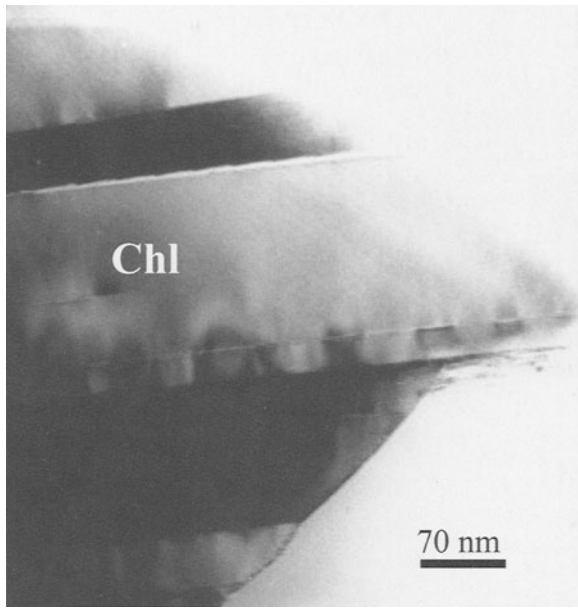

Figure 4. TEM lattice-fringe of sample DG-82, metabasite of pumpellyite-actinolite facies, showing defect-free, thick crystals of chlorite.

<10% interlayered smectitic and corrensitic layers, but the latter are less abundant than in the metabasalts. The expandable layers occur both as isolated smectite layers in chlorite or at boundaries of chlorite crystals (Figure 3b).

Diagenetic pelites. The texture of diagenetic pelites is very different from that of metabasites. In the lower-grade pelites, chlorite and berthierine are the main trioctahedral phyllosilicates, but they coexist with illite and mixed-layered illite-smectite (I-S) which are the dominant clay minerals. The general texture is defined by small packets of phyllosilicates, mainly dioctahedral illite and I-S, but with some 'chlorite' that fills the pore-space between larger detrital grains. Illite and (R = 3) I-S with thickness <500 Å are the main dioctahedral phyllosilicates. Large (>200 nm thick) $2M_1$ detrital muscovite was observed also. Smectitic (saponitic) mixed layers are much less abundant in chlorite of metapelites than in the metabasites, berthierine being the principal mixed-layered component in 'chlorite'. Figure 3c and 3d are TEM images of a diagenetic pelite from the Szarvaskö complex. Figure 3c shows a typical texture of a low-grade metapelite where illite packets <500 Å thick and I-S crystals occur. Chlorite (~500 Å thick) shows straight layers in defect-free crystals with low-angle contacts with illite. Interstratification of Fe-rich berthierine and chlorite layers, Fe-rich berthierine and 10 Å layers, and 14+7 Å layers with 10 Å layers were observed in the lower-grade pelites. The Fe-rich berthierine also occurs as separate small packets, or within large packets that are dominated by chlorite layers, or individual crystals up to 50 nm thick. Figure 3d shows a TEM image of packets of individual crystals of berthierine and illite crystals. As indicated by SAED patterns, berthierine and illite crystals are parallel and show characteristic 7 and 10 Å periodicities. No chlorite layers are present in berthierine, but rare 10 Å layers were detected within the berthierine packets. Figure 3e shows a SAED pattern of typical, interstratified chlorite-berthierine, with illite. Prominent streaking occurs along c*, even-order 00l reflections based on 14 Å periodicity being strong and sharp, whereas odd-order reflections are weak and diffuse. Lastly, μm-thick chlorite and muscovite crystals were detected, such crystals having the large size, angular outlines and ideal structures typical of detrital material derived from higher-grade rocks.

Pumpellyite-actinolite and greenschist-facies metabasites. Figures 4, 5 and 6 show chlorite crystals of metabasites and metapelites from pumpellyite-actinolite to greenschist facies (*i.e.* from high-anchizonal to epizonal grades). Chlorite in higher-grade, strongly recrystallized metabasites occurs as large, well crystallized crystals in interlocking textures with feldspars and other phyllosilicates. Muscovite crystals ($2M_1$ polytype) occur as subparallel to parallel intergrowths with chlorite. Although chlorite crystallites are relatively perfect, kinking and/or bending occurs within some. Figure 4 shows a defect-free chlorite crystal from sample DG-82. Chlorite crystallites are parallel or at low angles to one another. Crystal thicknesses are between 40 and 1400 Å. Smectite (saponite) layers in chlorite are only rarely observed; 10 Å and 24 Å layers are occasionally observed at chlorite rims, and they are inferred to be due to retrograde effects (Mata *et al.,* 2000). Strain in the form of gliding along (00l) can be observed in Figure 4. Figure 5a and 5b show coeval pairs of chlorite crystals from greenschist-facies meta-andesite tuff (DG-68) and epizonal metapelite (Dt-8, 118 m). Chlorite in sample DG-68 occurs as large (>1000 Å), defect-free crystallites showing low-angle boundaries. Some crystals have uncommon defects and intercalated 10 Å layers occur. Partially ordered stacking sequences of 3 to 4 units of 14 Å layers along c* can be seen, resulting in a SAED pattern showing streaking along c*. Muscovite of sample DG-68 occurs as thick and defect-free crystals (average thickness 3760 Å, with minimum values of 700 Å for n = 25 measurements) of the $2M_1$ polytype. Smectitic and I-S layers have been detected in the rims of >500 nm thick muscovite crystals, and are inferred to be a result of retrograde interaction with hydrothermal fluids.

Anchizonal and epizonal metapelites. Anchi- and epizonal metapelites contain coarse phyllosilicates, mainly $2M_1$ (>1000 Å thick) crystals of mica, in an interlocking texture. By comparison with the two lower-

https://doi.org/10.1346/CCMN.2001.0490406 Published online by Cambridge University Press

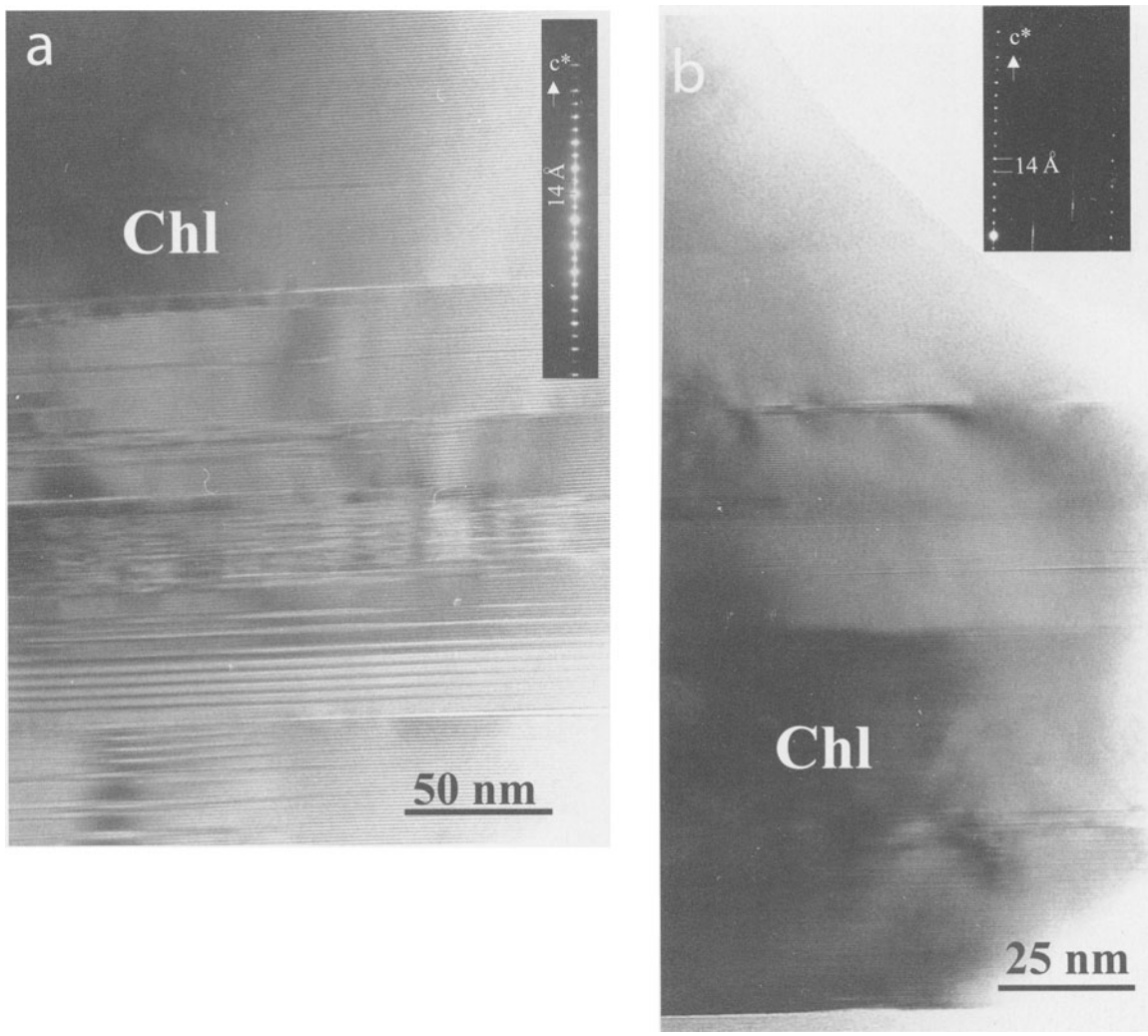

Figure 5. TEM lattice-fringe images of: (a) DG-68 (greenschist-facies meta-andesite tuff); and (b) Dt-8, 118 m (epizonal metapelite). Both show thick parallel crystals and stacking faults.

grade samples, intergrown chlorite and mica packets are composed of straight layers, are thicker, and display low-angle grain boundaries. Chlorite from the DG-73 metapelite shows large defect-free crystals with rare 10 Å layers. Superstructure reflections were observed along c* in SAED patterns lacking non-00*l* reflections. Therefore they are not caused by dynamic diffraction and thus reflect semi-random stacking. In metapelite Dt-8 118 m, large (>1000 Å thick) crystals are defect-free and have non-periodic stacking as well (Figure 5b). The SAED pattern shows satellite reflections in the 0*kl* row, $k \neq 3n$, indicating a long-period order that is not observed in the TEM lattice-fringe image. Epizonal mica crystals of this sample average 2100 Å in thickness (σ = 1481 for n = 40 measurements). Figure 6 is a TEM lattice-fringe image of sample Dt-8, 207.5 m, showing characteristic features of the epizonal metasandstone. Chlorite occurs as thick, defect-free crystals, with straight 14 Å fringes. These characteristics are common in both metabasites and metapelites.

Evolution of crystallite thickness of chlorite

A detailed study by Árkai *et al.* (2000) of these samples showed that mean crystallite thicknesses of chlorite from coeval pairs of metapelites and metabasites are similar, and the histograms of chlorite thicknesses, as measured by TEM, are positively skewed. In the lower-grade metabasites most of the chlorite crystallites are between 200 and 600 Å thick, with an average value of ~400 Å for both metapelites and metabasites, and with a median value of ~300 Å. In the diagenetic metapelites, most of the chlorite crystallites are <600 Å thick; the mean values for DG-62 and DG-20 are 520 Å and 590 Å, respectively. We emphasize that in metape-

https://doi.org/10.1346/CCMN.2001.0490406 Published online by Cambridge University Press

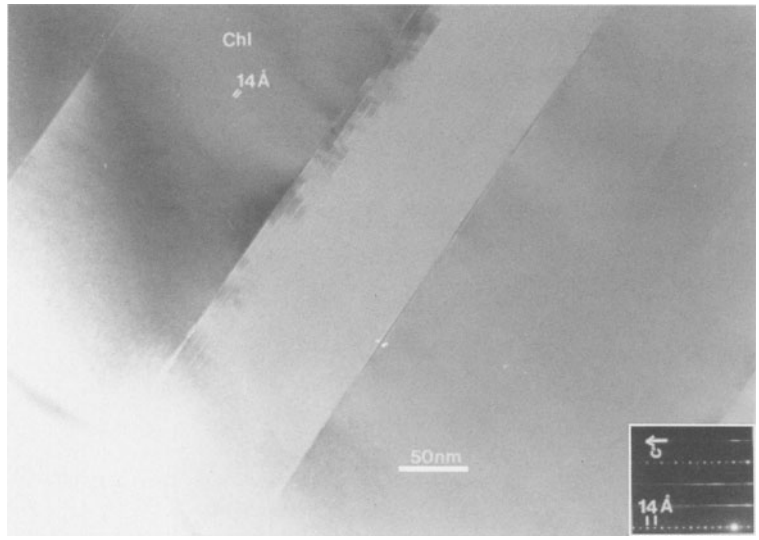

Figure 6. TEM lattice-fringe image of sample DT-8, 207.5 m (epizonal sandstone) showing 14 Å spacings of thick, defect-free, parallel chlorite crystals.

lites, no large (μm-size) detrital grains have been included in these mean values, *i.e.* they correspond only to authigenic crystallites. On the other hand, illite crystallite thicknesses in lower-grade metabasite sample DG-33 have a mean value of 205 Å (n = 8) whereas diagenetic metapelites have a mean value of 540 Å (with maximum and minimum values of 7100 and 350 Å, respectively).

Chlorite from pumpellyite-actinolite facies and transitional anchi-, epizonal samples DG-82 and DG-73 has mean thicknesses of 1150 Å and 1650 Å, respectively, whereas illite crystallite thicknesses have a mean value of 2666 Å (11,000 and 340 Å as maximum and minimum values). As grade increases, mean crystallite thickness values increase, both for chlorite and illite in metabasalts and metapelites. Thus, greenschist facies and epizonal samples have mean values of 1656 Å and 2658 Å for chlorites of metabasites Dt-8, 129.5 m and DG-68, and 2131 Å and 2667 Å for chlorites of metapelites Dt-8, 207.8 m and Dt-8, 118 m. Illite crystallite thicknesses increase too. For metabasite DG-68 the mean value is 3741 Å with a maximum of 9600 and a minimum of 660 Å, and for epizonal metapelite the values are 2091 Å, 7100 Å and 350 Å, respectively.

Chemical composition of chlorite

Representative chemical compositions of chlorite from metabasites and metapelites determined by AEM are given in Table 2. Formulae are normalized to an

Table 2. Representative normalized analytical electron microscope (AEM) data for chlorite. Normalization is based on 12 total cations. All Fe is assumed to be ferrous. FM: Fe^{2+}/Fe^{2+} + Mg. Metasedimentary rock units in italics.

									Dt-8		
Sample	DG-56	*DG-62*	DG-33	*DG-20*	DG-16	DG-82	*DG-73*	DG-68	*118.0*	129.5	*207.8*
Si	6.61	5.71	6.14	5.20	5.75	5.89	5.51	5.72	5.48	5.86	6.22
Al^{IV}	1.39	2.29	1.86	2.80	2.25	2.11	2.49	2.28	2.52	2.14	1.78
Al^{T}	3.86	4.31	4.27	5.97	4.75	4.38	5.03	4.67	5.90	4.85	4.26
Al^{VI}	2.47	2.02	2.41	3.17	2.50	2.27	2.54	2.39	3.38	2.71	2.47
Ti	0.00	0.00	0.00	0.00	0.00	0.00	0.00	0.00	0.00	0.00	0.00
Fe^{2+*}	3.98	4.64	5.42	6.35	4.56	3.49	4.50	6.25	5.28	7.56	3.51
Mg	5.44	4.96	4.06	1.99	4.76	6.05	4.87	2.96	3.22	1.72	6.02
Mn	0.11	0.26	0.11	0.36	0.19	0.19	0.10	0.40	0.12	0.00	0.00
Cr	0.03	0.12	0.00	0.12	0.00	0.00	0.00	0.00	0.00	0.00	0.00
Σ Oct.	12	12	12	12	12	12	12	12	12	12	12
Ca	0.12	0.00	0.30	0.00	0.00	0.00	0.00	0.00	0.00	0.12	0.00
Na	0.00	0.00	0.00	0.00	0.00	0.00	0.00	0.00	0.00	0.00	0.00
K	0.00	0.26	0.00	0.00	0.00	0.00	0.00	0.00	0.00	0.00	0.00
Σ Int.	0.12	0.26	0.30	0.00	0.00	0.00	0.00	0.00	0.00	0.12	0.00
Total	20.12	20.26	20.30	20	20	20	20	20	20	20.12	20
FM	0.42	0.48	0.57	0.76	0.49	0.37	0.48	0.68	0.62	0.81	0.37

https://doi.org/10.1346/CCMN.2001.0490406 Published online by Cambridge University Press

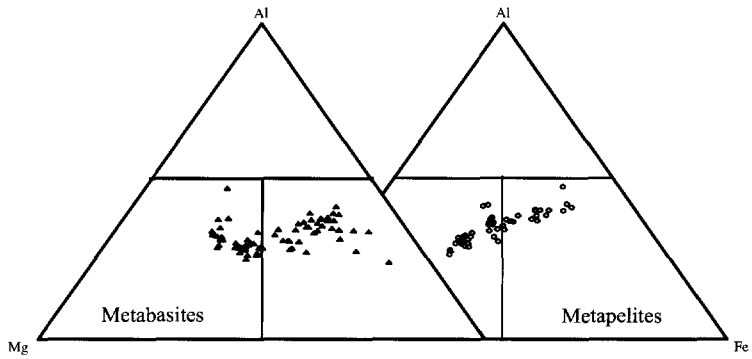

Figure 7. Plots of chlorite composition from metabasites (triangles) and metapelites (circles) using the classification scheme for rock-forming chlorite according to Zane and Weiss (1998). Points as defined by Wiewiora and Weiss (1990).

ideal trioctahedral formula with a total of 20 octahedral + tetrahedral cations. Iron was assumed to be ferrous. All normalized compositions correspond to a trioctahedral (tri-tri) structure. Figure 7 shows the Mg:Fe ratio *vs.* Si content, as proposed by Zane and Weiss (1998) as a basis of classification of rock-forming chlorite. All chlorite compositions plot as type I, *i.e.* where $X_{Mg} + X_{Fe_t} \geq X_{Al^{VI}} + X$, where X is the atomic fraction per formula unit. Although there is no clearly defined correspondence between rock type (metabasite *vs.* metapelite) and Mg : Fe ratio, chlorite from metabasites has a wider compositional range than chlorite from metapelites. Nevertheless, both show variable proportions of Fe : Mg and range from chamosite to clinochlore. The highest values of the Mg : Fe ratio of chlorite are, on first approximation, correlated with relatively high values of the Mg : Fe ratio of the corresponding rock (Árkai and Sadek Ghabrial, 1997) but there are exceptions. The formulae based on normalization to 20 cations, especially for lower-grade samples, are not charge-balanced, having $Al^{VI} > Al^{IV}$. Representative analyses of berthierine and chlorite crystals from diagenetic sample DG-20 are shown in Table 3. Differences in the Fe, Mg and Al contents occur, with $Fe^{2+}/(Fe^{2+} + Mg)$ and total Al content of berthierine being larger and smaller, respectively, than those of the chlorite.

Table 3. Representative AEM data for berthierine and chlorite from sample DG-20 (metapelite from the diagenetic zone). Normalization is based on 12 total cations. All Fe is assumed to be ferrous. FM: Fe^{2+}/Fe^{2+} + Mg.

	Bert.1	Bert.2	Chl
Si	4.55	5.20	6.31
Al^{IV}	3.45	2.80	1.69
Al^{T}	6.30	5.97	5.03
Al^{VI}	2.85	3.17	3.34
Fe^{2+}	6.32	6.35	5.20
Ti	0.00	0.00	0.00
Mg	2.12	1.99	3.17
Mn	0.70	0.36	0.28
Cr	0	0.12	0
Σ Oct.	12	12	12
Na	0	0	0
Ca	0	0	0.1
K	0	0	0
Σ Int.	0	0	0.1
Total	20	20	20.1
FM	0.74	0.76	0.62
Si/Al	0.7	0.87	1.25

DISCUSSION

The EM observations and AEM analyses define the evolution of chloritic material in coeval rock pairs of metabasites and metapelites for a range of grade from deep diagenesis to epizone. Because bulk compositions, textures, and original mineral assemblages of sediments and basalts were very different, we expected to observe rather different evolution paths. However, the data show that textural and mineralogical changes occur in a parallel way as a function of grade. The main features defining the similarity in the prograde sequence are a decrease in the percentage of interlayered material in both dioctahedral and trioctahedral phyllosilicates and increases in chlorite and illite crystallite thicknesses. The principal difference is in the type of mixed layering in the two rock types; in metabasites, smectite (saponite) is the principal mixed-layered component, whereas berthierine is the dominant component in metapelites, both smectite and berthierine being precursors to pure chlorite at higher grade. In the sections below, the occurrences of mixed-layering in the lowest-grade metabasites and metapelites are described, followed by a description of the full sequence of evolution of trioctahedral phases.

Occurrence of smectite-corrensite-chlorite in lower-grade metabasites

The lower-grade pillow basalt, DG-56 from the Darnó Hill complex, underwent prehnite-pumpellyite facies ocean-floor hydrothermal metamorphism, as did the pillow-structured metabasalt (DG-33) and

https://doi.org/10.1346/CCMN.2001.0490406 Published online by Cambridge University Press

metadiabase (DG-16) from the ophiolitic Szarvaskö complex. In the Szarvaskö complex, however, ocean-floor metamorphism was overprinted by orogenic anchizonal metamorphism (Sadek Ghabrial *et al.,* 1994, 1996; Árkai and Sadek Ghabrial, 1997). In these metabasites, 'chlorite' occurs as a secondary mineral both in the fine groundmass or as xenoblastic crystals replacing primary ferromagnesian minerals. No samples with discrete smectite were observed. Hydrothermal alteration of mid-ocean ridge basalt (MORB) occurs over the full range from saponite in shallow rocks through corrensite to chlorite in vertical sections (*e.g.* Shau and Peacor, 1992), and chlorite-rich samples of that sequence have been used extensively as a geothermometer (*e.g.* Cathelineau and Nieva, 1985). Discrete corrensite crystals (Figure 2) were found in the Darnó Hill sample, coexisting with discrete chlorite, as typical of the mid-depth of MORB alteration. The Darnó Hill sample is thus inferred to represent the mid-grade of the progression from smectite to chlorite in metabasites. The metabasalt (DG-33) and metadiabase (DG-16) from the Szarvaskö complex have a smaller proportion of corrensitic layers, however, as consistent with a higher grade imposed by regional metamorphic overprinting of the normal MORB alteration sequence. The decrease in percentage of expandable layers with advancing grade was also noted by Árkai and Sadek Ghabrial (1997) and Árkai *et al.* (2000) on the basis of the data obtained using the method of Bettison and Schiffman (1988) that determines the proportions of chlorite in chlorite-smectite mixed-layered material. Other studies have demonstrated that the percentage of expandable layers decreases in these systems with increasing T (or grade) also (Alt, 1999, and references therein).

There remain some questions as to whether or not there is a complete sequence of mixed-layered phases from saponite through chlorite, or whether or not discrete saponite, corrensite and chlorite occur as separate but coexisting pairs, as reviewed by Merriman and Peacor (1999 and references therein). In the case of the samples studied here, there is a clear distinction between packets of corrensite composed of sequences of alternating saponite- and chlorite-like layers, and chlorite. However, the corrensite commonly has extra chlorite layers and the chlorite invariably contains some saponite layers. Such relations are a direct consequence of the uniqueness and low relative free energy of the structure of corrensite relative to random mixed layering of saponite and chlorite layers.

The evolution of crystallite thicknesses of chlorite from lower-grade metabasites is discussed in Arkai *et al.* (2000). The average value is <50 nm but there is considerable scattering of values about the mean. The cause of the scatter is inferred to be due to two factors: (1) chlorite in metabasites occurs in a variety of modes, including groundmass, veins and replacements of primary ferromagnesian minerals; and (2) some samples have undergone more than one phase of metamorphism, and relict grains of an earlier phase may occur with those of a later event.

Occurrence of berthierine-chlorite in diagenetic pelites

'Chlorite' occurs both in coarse stacks with muscovite, and in the fine-grained matrices, in marked contrast to textures in the metabasites. According to the TEM observations, berthierine is the common mixed-layered phase found in the matrix, although mostly dioctahedral smectitic mixed layering also occurs as deduced from XRD and EMP data by Árkai *et al.* (2000). Berthierine occurs in lower-grade samples as discrete packets up to 500 Å thick which are commonly adjacent and sub-parallel to packets of diagenetic illite (Figure 3d) or I-S, or interstratified with chlorite (*e.g.* sample DG-20). Interlayering of small proportions of berthierine with chlorite may escape detection during routine mineralogical analysis but it has been reported through careful analysis with increasing frequency, especially in marine sediments (*e.g.* Curtis *et al.,* 1985; Ahn and Peacor, 1985; Amouric *et al.,* 1988; Hillier and Velde, 1992; Xu and Veblen, 1996). Recently, López-Munguira and Nieto (2000) and Schmidt *et al.* (1999) have also found interlayered berthierine, chlorite and saponite in diagenetic metasediments of volcanic origin. In these cases, chlorite contains mixed layers of smectite, but with less common occurrences of berthierine.

Berthierine has been inferred to be a metastable phase in most occurrences (*e.g.* Ahn and Peacor, 1985), forming within the stability field of chlorite at low temperatures where, through Ostwald-step-rule-like sequences, metastable intermediate phases commonly form (Essene and Peacor, 1997). Such metastable berthierine subsequently evolves to chlorite with increasing grade (Iijima and Matsumoto, 1982; Ahn and Peacor, 1985; Abad-Ortega and Nieto, 1995; Dalla Torre *et al.*, 1996; López-Munguira and Nieto, 2000). Although the number of observations of thickness of berthierine crystallites is relatively small, the average value ($\sim$<500 Å) is similar to the mean crystal thickness for chlorite in sample DG-20. Furthermore, parallel intergrowth of separate packets of berthierine and diagenetic I-S imply that they evolved in parallel at diagenetic grades. These data and the absence of berthierine in higher grade samples are thus consistent with a prograde sequence from berthierine to chlorite.

It has also been suggested that berthierine becomes more stable relative to chlorite with increasing proportion of Fe, and that Fe-rich berthierine

https://doi.org/10.1346/CCMN.2001.0490406 Published online by Cambridge University Press

may be a true polymorph of Fe-rich chlorite (chamosite). If so, Fe-rich berthierine may have a true stability field relative to chlorite. Some berthierine has been inferred to have the same composition as associated chlorite (Slack *et al.,* 1992; Jiang *et al.,* 1992; Xu and Veblen, 1996; Abad-Ortega and Nieto, 1995; López-Munguira and Nieto, 2000; Coombs *et al.,* 2000). Such pairs are therefore true polymorphs. On the other hand, other chlorite-berthierine pairs differ in X_{Mg} and X_{Al} content (Dalla Torre *et al.,* 1996), and are not polymorphs. Berthierine observed in this study is relatively Fe-rich, more so than coexisting chlorite. Therefore they are not polymorphs. Chemical analyses of bulk rock (Table 3 of Árkai *et al.,* 2000) show that the Fe content of berthierine-bearing sample DG-20 is the highest of the pelites. This implies that the occurrence of berthierine in the pelites is simply related to bulk-rock composition, being favored by relatively high Fe contents. This is also consistent with the lack of berthierine in the more Mg-rich metabasites, and the presence, rather, of mixed-layered phases with saponite-like layers. These data are in agreement with typical compositions of berthierine from marine-oolitic ironstone formations (Van Houten and Purucker, 1984), the occurrence of berthierine being consistent with such Fe-rich bulk compositions, or the presence of berthierine in metasediments of metavolcanic origin (López-Munguira and Nieto, 2000; Schmidt *et al.,* 1999). Whether it is metastable for all compositions relative to chlorite, or when Fe-rich it is a polymorph of chlorite and stable at lower temperatures than chlorite, is a question still to be answered. In any event, the berthierine occurring in the matrix as separate packets or as mixed layers with chlorite formed at relatively low temperatures and was replaced by chlorite at higher grades.

Chlorite was also detected in lower-grade pelites as chlorite-muscovite stacks, and may have a different origin from that of chlorite in the matrix. Further study is needed in order to characterize the structural and chemical features of these stacks, paying special attention to eventual differences from matrix phyllosilicates. Jiang and Peacor (1994b) and Li *et al.* (1994) described the sequence of alteration of detrital, volcanic biotite to stacks of chlorite and mica, with corrensite occurring as an intermediate phase. Although no relict biotite has been detected in the studied metapelites, acicular crystals of TiO_2 closely associated with the stacks may be interpreted as a key relation consistent with the relatively high Ti content of biotite. Although the origin of such stacks has been ascribed to many factors, as reviewed by Jiang and Peacor (1994b), the presence of TiO_2 implies that it originated from precursor biotite in this case also.

Evolution of chlorite with increasing metamorphic grade in metabasites and metapelites

With increasing metamorphic grade, the proportions of mixed layering decrease both in illite-muscovite and chlorite of both metabasites and metapelites. Chlorite from higher-grade anchizonal and epizonal metapelites and pumpellyite-actinolite and greenschist-facies metabasites occurs as thick sequences of parallel 14 Å layers with few defects. Layer terminations are scarce, and random or semi-random stacking sequences, which are generally common in chlorite, are present as indicated in SAED patterns by complete streaking of rows with $k \neq 3n$. Similar textural characteristics have been observed in coeval pairs of rocks: both the mean crystallite thickness values and the homogeneity of chlorite crystals increase with advancing grade. On the other hand, planar stacking faults and isolated 9 or 7 Å layers are common features of higher-grade chlorite. These spacings have been interpreted as interlayered 1:1 phyllosilicates and a chlorite unit where a brucite sheet was removed, respectively (Bons and Schryvers, 1989). Bons (1988) studied deformation structures of chlorite by HRTEM and suggested a deformation-induced origin for these features. Deformation features are more abundant in the higher-grade rocks of this study, and there are more deformation features in chlorite than in muscovite, probably due to the fact that chlorite tends to retain defects and lattice strain, in comparison with muscovite (Merriman *et al.,* 1995; Árkai *et al.,* 1996). Such relations are consistent with Bons' (1988) suggestion that the rare mixed layering is an artifact of deformation, and thus has a very different origin than mixed layering in low-grade rocks, which originates through neocrystallization of metastable phases.

Relic mixed layering is absent in the epizonal and greenschist-facies samples of borehole Dt-8 and the Bükk Mountains, but minor berthierine occurs on the rims of larger chlorite crystals. Likewise, smectite and I-S occur at the rims of muscovite crystals, both in metabasites and metapelites. These textural relations are in marked contrast with mixed layering or the occurrence of separate packets, as described above for prograde relations. They are instead inferred to be due to retrograde overprinting, as they occur only at crystal rims, and never as layers within crystals. Such retrograde overprinting, due to interaction with fluids, has been proposed to explain the berthierine associated with a massive sulphide deposit in Ontario by Jiang *et al.* (1992). Such retrograde alteration of illite and muscovite, with textures similar to those of the samples of this study is not unusual; it cannot generally be detected by XRD, but has been recognized with increasing fre-

https://doi.org/10.1346/CCMN.2001.0490406 Published online by Cambridge University Press

quency with the application of TEM (*e.g.* Nieto *et al.,* 1994; Zhao *et al.,* 1999; Mata *et al.,* 2000).

Chlorite (*sensu stricto*) thickness and texture evolve similarly in coeval metabasites and metasediments, which is somewhat surprising given the differences in bulk rock compositions, textures and primary minerals. It is perhaps even more surprising in that the kinds of mixed layering are very different in the two rock types. As noted above, however, the occurrence of berthierine in pelites is an apparent expression of the greater proportions of Fe in such rocks. Trioctahedral smectite, on the other hand, is invariably relatively Mg-rich. The occurrence of mixed-layered smectite (saponite)-chlorite is therefore compatible with the more Mg-rich bulk rock composition of metabasites. In addition to berthierine, mixed layering of smectite in chlorite also occurs in the metasediments studied. Such mixed layering has been interpreted to be the principal cause of variations in so-called chlorite which have been correlated with temperature of formation (Jiang and Peacor, 1994a). Whether the mixed layering involves berthierine or smectite, however, such phases are thermodynamically metastable, and their occurrence can be ascribed only to reaction progress, and are not a quantitative function of temperature (Essene and Peacor, 1995).

Árkai *et al.* (2000) pointed out that reaction progress in metapelites, measured in part by chlorite crystallinity, paralleled that in metabasites. The data of this study show that chlorite crystals from both metabasites and metapelites become larger and display fewer defects, with a general simplification in microtextural relations as grade increases. This is illustrated in part by the decrease in the number of mineral species with increasing grade, chlorite being the only trioctahedral mineral at higher grades. This is consistent with the reaction progress trend where both metastable systems (metabasites and metapelites) tend toward the same end-member, thermodynamically stable chlorite, as well as texture (crystal size), and that all the intermediate states are metastable, and controlled by the Ostwald step rule (Merriman and Peacor, 1999). According to the Ostwald step rule, the original metastable assemblage, berthierine-smectite-corrensite-chlorite will change via reactions towards the stable state, represented by large crystals of pure chlorite, the small number of phases of relatively large crystal size being consistent with the Gibbs phase rule.

ACKNOWLEDGMENTS

This research was partially supported by National Science Foundation grants EAR 9418108 and EAR 9814391 to D.R.P. and by the Hungarian National Research Fund (OTKA, Budapest), project No. T-022773/1997–2000 to P.Á. We thank L.-S. Kao and C. Henderson for technical assistance. The original version of the manuscript was improved by the constructive reviews of L. Bettison-Varga and R.E. Bevins.

REFERENCES

Abad-Ortega, M.M. and Nieto, F. (1995) Genetic and chemical relationships between berthierine, chlorite and cordierite in nodules associated to granitic pegmatites of Sierra Albarrana (Iberian Massif, Spain). *Contributions to Mineralogy and Petrology,* **120,** 327–336.

Ahn, J.H. and Peacor, D.R. (1985) Transmission electron microscopic study of diagenetic chlorite in Gulf Coast argillaceous sediments. *Clays and Clay Minerals,* **33,** 228–236.

Alt, J.C. (1999) Very low-grade hydrothermal metamorphism of basic igneous rocks. Pp. 169–226 in: *Low-Grade Metamorphism* (M. Frey and D. Robinson, editors). Blackwell Science, Oxford.

Amouric, M., Gianetto, I. and Proust, D. (1988) 7, 10 and 14 Å mixed-layer phyllosilicates studied structurally by TEM in pelitic rocks of the Piemontese zone (Venezuela). *Bulletin Mineralogique,* **111,** 29–37.

Árkai, P. (1983) Very low- and low-grade Alpine regional metamorphism of the Paleozoic and Mesozoic formations of the Bükkium, NE-Hungary. *Acta Geologica Hungarica,* **26,** 83–101.

Árkai, P. (1991) Chlorite crystallinity: An empirical approach and correlation with illite crystallinity, coal rank and mineral facies as exemplified by Palaeozoic and Mesozoic rocks of northeast Hungary. *Journal of Metamorphic Geology,* **9,** 723–734.

Árkai, P. and Sadek Ghabrial, D. (1997) Chlorite crystallinity as an indicator of metamorphic grade of low-temperature meta-igneous rocks: A case study from the Bükk Mountains, northeast Hungary. *Clay Minerals,* **32,** 205–222.

Árkai, P. and Tóth, M. (1990) Illite and chlorite "crystallinity" indices, I: an attempted mineralogical interpretation. *Conference on "Phyllosilicates as indicators of very low-grade metamorphism and diagenesis".* IGCP 294, Manchester, Abstract.

Árkai, P., Balogh, K. and Dunkl, I. (1995) Timing of low-temperature metamorphism and cooling of the Paleozoic and Mesozoic formations of the Bükkium, innermost Western Carpathians, Hungary. *Geologische Rundschau,* **84,** 334–344.

Árkai, P., Mata, M.P., Giorgetti, G., Peacor, D.R. and Tóth, M. (2000) Comparison of diagenetic and incipient metamorphic evolution of chlorites in associated pelitic sedimentary and basic igneous rocks: An integrated TEM and XRD study. *Journal of Metamorphic Geology,* **18,** 531–550.

Bettison, L.A. and Schiffman, P. (1988) Compositional and structural variations of phyllosilicates from the Point Sal ophiolite, California. *American Mineralogist,* **73,** 62–76.

Bons, A.J. (1988) Deformation of chlorite in naturally deformed low-grade rocks. *Tectonophysics,* **154,** 149–165

Bons, A.J. and Schryvers, D. (1989) High-resolution electron microscopy of stacking irregularities in chlorites from the central Pyrenees. *American Mineralogist,* **74,** 1113–1123.

Bucher, K. and Frey, M. (1994) *Petrogenesis of Metamorphic Rocks, 6th edition.* Complete revision of Winkler's textbook. Springer-Verlag, Berlin.

Cathelineau, M. and Nieva, D. (1985) A chlorite solid solution geothermometer. The Los Azufres (Mexico) geothermal system. *Contributions to Mineralogy and Petrology,* **91,** 235–244.

Coombs, D.S., Zhao, G. and Peacor, D.R. (2000) Manganoan berthierine, Meyers Pass, New Zealand: Occurrence in the prehnite-pumpellyite facies. *Mineralogical Magazine,* **64,** 1037–1046.

Curtis, C.D., Hughes, C.R., Whiteman, J.A. and Whittle, C.K. (1985) Compositional variations within some sedimentary

https://doi.org/10.1346/CCMN.2001.0490406 Published online by Cambridge University Press

chlorites and some comments on their origin. *Mineralogical Magazine,* **49,** 375–386.

Dalla Torre, M., Livi, K.J.T. and Frey, M. (1996) Chlorite textures and compositions from high-pressure/low-temperature metashales and metagraywackes, Franciscan Complex, Diablo Range, California, USA. *European Journal of Mineralogy,* **8,** 825–846.

Downes, H., Pantó, Gy., Árkai, P. and Thirlwall, M.F. (1990) Petrology and geochemistry of Mesozoic igneous rocks, Bükk Mountains, Hungary. *Lithos,* **24,** 201–215.

Essene, E.J. and Peacor, D.R. (1995) Clay mineral thermometry—a critical perspective. *Clays and Clay Minerals,* **43,** 540–553.

Frey, M. (1987) Very low-grade metamorphism of clastic sedimentary rocks. Pp. 9–58 in: *Low Temperature Metamorphism* (M. Frey, editor). Blackie, Glasgow and London, UK.

Hillier, S. (1993) Origin, diagenesis, and mineralogy of chlorite minerals in Devonian lacustrine mudrocks, Orcadian Basin, Scotland. *Clays and Clay Minerals,* **41,** 240–259.

Hillier, S. (1994) Pore-lining chlorites in siliciclastic reservoir sandstones: electron microprobe, SEM and XRD data, and implications for their origin. *Clay Minerals,* **29,** 665–679

Hillier, S. and Velde, B. (1992) Chlorite interstratified with a 7 Å mineral: an example from offshore Norway and possible implications for the interpretation of the composition of diagenetic chlorites. *Clay Minerals,* **27,** 475–486.

Ijima, A. and Matsumoto, R. (1982) Berthierine and chamosite coal measures of Japan. *Clays and Clay Minerals,* **30,** 264–274.

Jiang, W.T. and Peacor, D.R. (1994a) Prograde transitions of corrensite and chlorite in low-grade pelitic rocks from Gaspe Peninsula, Quebec. *Clays and Clay Minerals,* **42,** 497–517.

Jiang, W.T. and Peacor, D.R. (1994b) Formation of corrensite, chlorite and chlorite mica stacks by replacement of detrital biotite in low-grade pelitic rocks. *Journal of Metamorphic Geology,* **12,** 867–884.

Jiang, W.T., Peacor, D.R., Merriman, R.J. and Roberts, B. (1990) Transmission and analytical electron microscopic study of mixed-layer illite/smectite formed as an apparent replacement product of diagenetic illite. *Clays and Clay Minerals,* **38,** 449–468.

Jiang, W.T., Peacor, D.R. and Slack, J.F. (1992) Microstructures, mixed layering, and polymorphism of chlorite and retrograde berthierine in the Kidd Creek massive sulphide deposit, Ontario. *Clays and Clay Minerals,* **40,** 501–514.

Jiang, W.-T., Peacor, D.R. and Buseck, P.R. (1994) Chlorite geothermometry?—contamination and apparent octahedral vacancies. *Clays and Clay Minerals,* **42,** 593–605.

Kovács, S. (1989) Major events of the tectono-sedimentary evolution of the North Hungarian Paleo-Mesozoic: history of the northwestern termination of the Late Paleozoic–Early Mesozoic Tethys. Pp. 93–108 in: *Tectonic Evolution of the Tethyan Region* (A.M.C. Sengor, editor). Kluwer Academic Publishers, Dordrecht.

Kovács, S., Szederkényi, T., Árkai, P., Buda, Gy., Lelkes-Felvári, Gy. and Nagymarosi, A. (1996–97) Explanation to the terrane map of Hungary. *Annales Géologiques des Pays Helléniques,* **37,** 271–330.

Laird, J. (1988) Chlorites: Metamorphic petrology. Pp. 405–453 in: *Hydrous Phyllosilicates* (P.H. Ribbe, editor). Reviews in Mineralogy, **19.** Mineralogical Society of America, Washington, D.C.

Lee, J.H. and Peacor, D.R. (1983) Intralayer transitions in phyllosilicates of the Martinsburg Shale. *Nature,* **303,** 608–609.

Li, G., Peacor, D.R., Merriman, R.J., Roberts, B. and van der Pluijm, B.A. (1994) TEM and AEM constraints on the origin and significance of chlorite-mica stacks in slates: An example from Central Wales, U.K. *Journal of Structural Geology,* **16,** 1139–1157.

Li, G., Peacor, D.R. and Coombs, D.S. (1997) Transformation of smectite to illite in bentonite and associated sediments from Kaka point, New Zealand: contrast in rate and mechanism. *Clays and Clay Minerals,* **45,** 54–67.

López-Munguira, A. and Nieto, F. (2000) Transmission electron microscopy study of very-low grade metamorphic rocks in Cambrian sandstones and shales, Ossa-Morena zone, Southwest Spain. *Clays and Clay Minerals,* **48,** 213–223.

Masuda, H., O'Neil, J.R., Jiang, W.-T. and Peacor, D.R. (1996) Relation between interlayer composition of authigenic smectite, mineral assemblages, I/S reaction rate and fluid composition in silicic ash of the Nankai Trough. *Clays and Clay Minerals,* **44,** 460–469.

Mata, M.P., Arkai, P., Giorgetti, G. and Peacor, D.R. (2000) Retrogression of metamorphic phyllosilicates in low-grade rocks. *31st International Geological Congress* (Brazil, 2000).

Merriman, R.J. and Frey, M. (1999) Patterns of very low-grade metamorphism in metapelitic rocks. Pp. 61–107 in: *Low-Grade Metamorphism* (M. Frey and D. Robinson, editors). Blackwell Science, Oxford.

Merriman, R.J. and Peacor, D.R. (1999) Very low-grade metapelites: Mineralogy, microfabrics and measuring reaction progress. Pp. 10–60 in: *Low-Grade Metamorphism* (M. Frey and D. Robinson). Blackwell Science, Oxford.

Merriman, R.J. Roberts, B., Peacor, D.R. and Hirons, S.R. (1995) Strain-related differences in the crystal growth of white mica and chlorite: A TEM and XRD study of the development of metapelite microfabrics in the Southern Uplands thrust terrane, Scotland. *Journal of Metamorphic Geology,* **13,** 559–576.

Morse, J.S. and Casey, W.H. (1988) Ostwald processes and mineral paragenesis in sediments. *American Journal of Science,* **288,** 537–560.

Nieto, F., Velilla, N., Peacor, D.R. and Huertas, M. (1994) Regional retrograde alteration of sub-greenschist facies chlorite to smectite. *Contributions to Mineralogy and Petrology,* **115,** 243–252.

Robinson, D. and Bevins, R.E. (1999) Patterns of regional low-grade metamorphism in metabasites. Pp. 143–168 in: *Low-Grade Metamorphism* (M. Frey and D. Robinson, editors). Blackwell Science, Oxford.

Robinson, D. and Merriman, R.J. (1999) Low-temperature metamorphism: An overview. Pp. 1–9 in: *Low-Grade Metamorphism* (M. Frey and D. Robinson, editors). Blackwell Science, Oxford.

Sadek-Ghabrial, D., Árkai, P. and Nagy, G (1994) Magmatic features and metamorphism of plagiogranite associated with a Jurassic MORB-like basic-ultrabasic complex, Bükk Mountains, Hungary. *Acta Mineralogia et Petrographia Szegediensis,* **35,** 41–69.

Sadek-Ghabrial, D., Árkai, P. and Nagy, G. (1996) Alpine polyphase metamorphism of the ophiolitic Szarvaskõ complex, Bükk Mountains, Hungary. *Acta Mineralogia et Petrographia Szegediensis,* **37,** 99–128.

Schiffman, P. and Day, H.W. (1999) Petrological methods for the study of very low-grade metabasites. Pp. 18–142 in: *Low-Grade Metamorphism* (M. Frey and D. Robinson, editors). Blackwell Science, Oxford.

Schmidt, D., Livi, K.J.T. and Frey, M. (1999) Reaction progress in chloritic mineral: An electron microbeam study of the Taveyanne greywacke, Switzerland. *Journal of Metamorphic Geology,* **17,** 229–241.

Shau, Y.-H. and Peacor, D.R. (1992) Phyllosilicates in hydrothermally altered basalts from DSDP hole 504B, leg 83 a

https://doi.org/10.1346/CCMN.2001.0490406 Published online by Cambridge University Press

TEM and AEM study. *Contributions to Mineralogy and Petrology,* **112,** 119–133.
Slack, J.F., Jiang, W.T., Peacor, D.R. and Okita, P.M. (1992) Hydrothermal and metamorphic berthierine from the Kidd Creek volcanogenic massive sulphide deposit, Timmins, Ontario. *Canadian Mineralogist,* **30,** 1127–1142.
Van Houten, F.B. and Purucker, M.E. (1984) Glauconitic peloids and chamositic ooids—favorable factors, constraints, and problems. *Earth Science Reviews,* **20,** 211–243.
Wiewióra, A. and Weiss, Z. (1990) Crystallochemical classification of phyllosilicates based in the unified system of projection of chemical composition. II. The chlorite group. *Clay Minerals,* **25,** 83–92.
Xu, H. and Veblen, D.R. (1996) Interstratification and other reaction microstructures in the chlorite-berthierine series. *Contributions to Mineralogy and Petrology,* **124,** 291–301.
Zane, A and Weiss Z. (1998) A procedure for classification of rock-forming chlorites based on microprobe data. *Rend. Fis. Accad. Lincei,* **9,** 51–56.
Zhao, G., Peacor, D.R. and McDowell, S.D. (1999) Retrograde diagenesis of Clay Minerals of the Freda Sandstone, Wisconsin. *Clays and Clay Minerals,***47,** 119–130.

E-mail of corresponding author: pilar.mata@uca.es
(Received 23 September 2000; revised 3 January 2001; Ms. 489; A.E. Warren D. Huff)

https://doi.org/10.1346/CCMN.2001.0490406 Published online by Cambridge University Press